Mathematical Modelling and Control

http://www.aimspress.com/journal/mmc

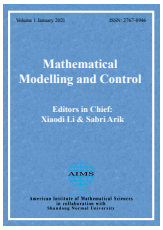

MMC, 5(4): 338–354.
DOI: 10.3934/mmc.2025023
Received: 19 October 2023
Revised: 30 August 2024
Accepted: 24 October 2024
Published: 15 October 2025

Research article

Combined effects of antipredator behaviors and cooperative hunting in a stage-structured predator-prey model

Ankur Jyoti Kashyap[1,5,*], **Fengde Chen**[2], **Fanitsha Mohan**[3], **Anuradha Devi**[3] **and Hemanta Kumar Sarmah**[4]

[1] Department of Mathematics, Girijananda Chowdhury University, Guwahati, 781017, India

[2] School of Mathematics and Statistics, Fuzhou University, Fuzhou 350108, China

[3] Department of Mathematics, The Assam Royal Global University, Guwahati, 781035, India

[4] Department of Mathematics, Gauhati University, Guwahati, 781014, India

[5] Center for Wildlife and Environmental Studies, Girijananda Chowdhury University, Guwahati, 781017, India

* **Correspondence:** Email: ajkashyap.maths@gmail.com.

Abstract: Collaborative hunting among predators is a common strategy that significantly improves the efficiency of the hunting process by increasing prey fear, consequently impacting their reproduction rate. This work investigated a predator-prey interaction system with a stage-structured prey population. The conversion from juvenile to matured prey was assumed to be density-dependent. We also assumed that predators benefit from hunting cooperation and that mature prey are capable of defending in groups against predators. All possible biologically feasible equilibrium states of the model were determined, and their stabilities were analyzed. The role of various important factors, e.g., hunting cooperation rate, predation rate, and rate of fear, on the system dynamics were discussed. Populations within the ecosystem exhibit chaotic dynamics with varying predator mortality rates. In addition, a stable stock of predator population was observed with its increasing mortality rate, showing a positive hydra effect.

Keywords: hunting cooperation; stage structure; Hopf bifurcation; hydra effect; numerical simulation

1. Introduction

In the twenty-first century, mathematical models have gained popularity and value for explaining population dynamics [1]. The process of mathematical modelling involves transforming a real-world problem into mathematical language, generally in the form of equations, and using those equations to both understand the problem at hand and uncover new elements of it. Examining the numerous processes implicated in the interaction between predators and prey stands as a central concern within the fields of ecology and evolutionary biology [2]. The process of predation plays a crucial role in accelerating life's evolution and preserving ecological harmony and biodiversity. Predation is the act of consuming all or a portion of the body of a prey organism. Population dynamics of predator and prey are influenced by one another [3]. The complex relationship between a predator and its prey has been well-established since the 18th century due to its widespread existence and supremacy, and has become a significant factor in ecosystem studies. Recent experimental results on terrestrial vertebrates revealed that the fear of predation risks significantly impacts the prey's lifestyle, indirectly decreasing their reproduction rate. Preys frequently alter their habitats, their foraging strategies, vigilance, and different physiological changes occur as anti-predator responses [3–7]. According to reports by Zanette et al. [8], the song sparrow's perpetuation was lowered by 40% as a response to the predators' incited dread. Based on all of these testimonies, system dynamics should take

into account both the direct influence of predators like predation and their indirect effects. In another experiment, Elliott et al. [9] reported that *Drosophila melanogaster* showed anti-predator behaviors when exposed to the odor of a *mantid*, including reduced activity in all breeding as well as non-breeding seasons. Based on the experimental results on song sparrows, Wang et al. [10] took into account a mathematical prey-predator model considering the fear risk and revealed that high levels of fear could stabilize the ecosystem by excluding the appearance of periodic oscillations of the population. Cooperation stands as a crucial aspect of the social lives of animals and holds significant importance within biological systems. In the context of hunting, cooperation refers to the collaboration of two or more individuals, regardless of their relatedness, as they work together to enhance their fitness by jointly pursuing a shared goal. Predators can attack either lone or clustered prey in a coordinated and collective manner. While hunting, some predators in ecosystems follow a cooperation strategy to increase their chances of success and induce dread in their prey. For instance, wolves, during hunting in groups, impose an indirect effect on their prey [11, 12]. As anti-predator measures, elk avoid habitats frequented by wolves [13]. When wolves are in the vicinity, elk become even more sensitive to their surroundings [4, 14]. Stander [15] observed that during group hunting, a strategy employed by some lionesses involved encircling the prey, while others opted for a patient stance, awaiting the prey's approach. In this context, many scientists used mathematical models to examine the effects of hunting cooperation and fear effect in predator-prey systems separately. Duarte et al. [16] evaluated the dynamics of cooperative hunting in a McCann and Yodzis food web model with three different species. Berec [17], in a modified Rosenzweig-MacArthur model, explored foraging facilitation among predators and revealed that foraging facilitation could destabilize predator-prey dynamics. Saha et al. [18] explored a tri-trophic food-chain model with a Holling type-III functional response, revealing that prey refuges can paradoxically bring stability or instability to the system. Considering a communicable disease, the same authors examined another model utilizing hunting cooperation and group defense mechanisms in [19]. Using an extended Lotka-Volterra model that considers predator-hunting cooperation, Alves and Hilker [20] investigated how cooperation affects predator-prey dynamics. Their findings indicated that hunting cooperation gives rise to Allee effects within predator populations. Considering the combined fear due to hunting cooperation, Pal et al. [3] explored the predator-prey dynamics by extending a modified Lotka-Volterra model and reported that with an increase in the hunting cooperation rate, the induced fear could destabilize the ecosystem. Extending their work, Kashyap et al. [21] studied a prey-predator model with Michaelis–Menten-type harvesting and found that the harvesting effort promotes stability to the coexistence of the populations. In population dynamics, prey often receive benefits by adopting another strategy, called a group defense. Due to the increase in prey's ability to protect or hide when they are in large numbers or groups, predation is reduced. For example, wolves prefer lone musk more than small herds (4–6) since larger herds are safer than smaller ones [22]. In recent decades, many natural populations, including birds, fish, and invertebrates, have been considered in the study of group defence and predation risk. Birds, e.g., sparrowhawks, *Accipiter nicus*, preying on redshanks, *Tringa tetanus* [23]; fishes, e.g., cichlids, *Aequidens pulcher* [24]; and other animals, e.g., lions, *Panthera leo*, preying on mixed ungulate herds [25] are considered in this context. As a defensive measure, Japanese honeybees construct to protect the hornet by creating a "hot defensive ball" [2, 26]. Freedman and Wolkowicz pioneered group defence in the mathematical modelling context in 1986 [27]. In general, Holling type-IV functional response or Monod-Haldane functional response are utilized to describe the group defence mechanism in mathematical models [2, 7, 27, 28]. Monod-Haldane functional response has the form $g(x) = \frac{p_0 x}{a_0+b_0 x+x^2}$, whereas the Holling type-IV function is the simplifed Monod-Haldane function of the form $g(x) = \frac{p_0 x}{a_0+x^2}$. Due to the presence of a square term, in the Holling type-IV response, the predator cannot survive above some upper threshold of prey density [29, 30]. Alves and Hilker suggested two modified versions of Holling type-II and type-IV function responses with hunting cooperation and group defence [20]. Much research has been carried out using mathematical modelling in recent years considering

the fear of predation risk and cooperative hunting [2, 3, 7].

Animals show different antipredator responses at different times during their life cycle. In recent years, significant research works have been carried out with stage-structured food web models. Stage-structured models are mathematical models used to study populations in which individuals are grouped into discrete age or stage classes. Most such models are mainly devoted to two stages, either in the prey or predator community. A recent experimental study by Griesser and Suzuki [31] revealed that predator functional responses are not identical for juvenile and adult birds. While adult birds exhibit various anti-predator responses upon detecting predation risk, juvenile birds lack the proficiency to display such responses [8]. Although adult prey gets benefits by showing anti-predator behaviors, the process requires extra energy and time. Repeated adaptations in anti-predator behavior indirectly affect the growth rate of the adult prey [4]. Therefore it is important to discuss a stage-structured model by incorporating anti-predator behavior. Panday et al. [32] presented a stage-structured model with two stages of the prey, juvenile and adult. Presuming the adult prey rely solely on group defence as an anti-predator mechanism, they showed that the absence of anti-predator behavior, combined with an increase in the maturation rate, can trigger a population cycle characterized by a sharp and significant increase in amplitude. This could potentially lead to the extinction of all species in the system. Panja et al. [33], in a stage-structured model with two stages in the prey, discussed the appearance of periodic orbits via Hopf bifurcation. Recently, in [1], Ghosh et al. presented a density-dependent stage-structured predator-prey model with two stages for both communities. In their study, Du et al. [34] introduced a predator-prey model featuring group defence behavior in prey and cooperative hunting behavior in predators. The model displays complex dynamics, including a bubble loop of limit cycles, as well as an open-ended branch of periodic orbits that disappear through either a homoclinic cycle or a loop of heteroclinic orbits. There are several models which considered anti-predator behaviors in prey, e.g., a fear effect, a group defence strategy, and hunting cooperation of predators [3, 7, 35–37].

The species mortality rate has a significant role in shaping predator-prey interactions. The traditional knowledge of the mortality rate of a species suggests that it decreases that particular biomass. New advancements in both theoretical and empirical research have brought to light the possibility that a species' mortality might not necessarily lead to a decrease in its own biomass [38–42]. Moreover, mortality could trigger a positive effect on the population of the same species. In recent years, many researchers have established the existence of this paradoxical effect in different stage-structured models, e.g., in [1], Ghosh et al. observed that stable stock on mature predator increases with its increasing mortality rate in a stage-structured prey-predator model with density-dependent effects in terms of prey reproduction and predator transition. This contradictory outcome has been termed the "hydra effect" by Abrams [39, 41].

All previously mentioned research pertains to models of predator-prey interactions that consider a combination of two factors, specifically the impact of fear, hunting cooperation, or group defence. To fully understand the dynamics of prey-predator interactions, it is critical to study how antipredator behaviors, including fear effects, group defence strategies, and predator-hunting cooperation, interact with stage structure in prey. To the best of our knowledge, no models have been introduced that take into account stage structure in prey alongside antipredator behaviors exhibited by prey and cooperative hunting strategies employed by predators. In the present investigation, we propose a predator-prey interaction model with two discrete stages in the prey: a juvenile stage and adult stage, where the predator population predates both stages of the prey. It is assumed that predators follow cooperative behavior during hunting which ultimately increases the fear of predation risk in the prey and affects its growth rate with a higher impact. We incorporate the benefit of group defence of adult prey in their predation term following two modified versions of Holling type-II and type-IV functions proposed by Alves and Hilker [20].

Our objective in this study is to investigate the effect of hunting cooperation, and the strength of fear, conversion rate, and predation rates on the population dynamics of the system. The findings of our study represent a significant contribution to the study of predator-prey interactions and

propose a novel and more complex model. In the next section, we formulate the mathematical model, and the basic mathematical results of the model are presented in Section 3. The local stability of the possible equilibrium states is analyzed in Section 4. Section 5 deals with the dynamical analysis of the system using bifurcation analysis. Using some hypothetical parameter values, the system is analyzed numerically for different possible bifurcations in Section 6. Finally, in Section 7, we end the paper with a discussion of our findings.

2. Model formulation

We consider an ecosystem with a single prey and a predator species where the prey species maintain their growth without predation. Depending on the ability to reproduce new offspring, we divide the prey species into two stages: juvenile and mature. For instance, consider $x(t)$ and $y(t)$ to represent juvenile prey and matured prey populations at time t, respectively, and $z(t)$ is the predator biomass at time t. Preys are capable of reproducing offspring only in a matured stage, and prey biomass is considered to be dependent on the reproduction rate, transfer rate (from juvenile to mature), and natural mortality rate. The conversion from juvenile to mature prey can be divided into two categories: density-independent and density-dependent. Abrams and Quince explored some more general models with density-dependent per capita growth rates of immature prey [43]. We assume that the transfer rate of juvenile prey to matured prey is density-dependent. The isoclines of prey and predator populations can be represented by the following two differential equations.

$$\begin{aligned} \frac{dx}{dt} &= ry - bx(1-\delta x) - d_1 x, \\ \frac{dy}{dt} &= bx(1-\delta x) - d_2 y, \end{aligned} \tag{2.1}$$

where $r > 0$ is the maximum per capita growth rate of the mature prey. $bx(1-\delta x)$ is the density-dependent transfer rate of immature prey to mature prey where $b > 0$ is the maximum per capita growth rate of the mature prey and $\delta > 0$ is the rate at which the per capita birth rate is decreased for the mature class with its increasing density. $d_1 > 0$ and $d_2 > 0$ are the natural mortality of the juvenile and matured prey, respectively.

Since fear due to predation risk indirectly reduces the reproduction rate, we modify (2.1) by multiplying the reproduction rate r by a factor $g(f,z)$ as follows:

$$\begin{aligned} \frac{dx}{dt} &= rg(f,z)y - bx(1-\delta x) - d_1 x, \\ \frac{dy}{dt} &= bx(1-\delta x) - d_2 y, \end{aligned} \tag{2.2}$$

where z denotes predator biomass and parameter f depicts the intensity of fear, which drives anti-predator behaviors of the prey. In biological aspects of $f, z, g(f,z)$, it is appropriate to assume:

$$\begin{aligned} &g(0,z) = 1, g(f,0) = 1, \lim_{f\to\infty} g(f,z) = 0, \\ &\lim_{z\to\infty} g(f,z) = 0, \frac{\partial g(f,z)}{\partial f} < 0, \frac{\partial g(f,z)}{\partial z} < 0. \end{aligned} \tag{2.3}$$

Here we consider $g(f,z) = (1+fz)^{-1}$ which satisfies condition (2.3). Then system (2.2) becomes

$$\begin{aligned} \frac{dx}{dt} &= \frac{ry}{1+fz} - bx(1-\delta x) - d_1 x, \\ \frac{dy}{dt} &= bx(1-\delta x) - d_2 y. \end{aligned} \tag{2.4}$$

We consider that, due to hunting cooperation, predators get benefits and success in capturing prey increases with predator density. A lot of recent studies paid attention to cooperative hunting among predators [20]. Alves and Hilker [20] considered the following types of predator-dependent functional response to model the cooperative hunting among predators based on the Holling type-II and type-IV functional responses.

$$\begin{aligned} \phi_1(x,z) &= \frac{(p_1+\alpha z)xz}{1+h_1(p_1+\alpha z)x}, \\ \phi_2(y,z) &= \frac{(p_2+\alpha z)yz}{1+h_2(p_2+\alpha z)y+h_3(p_2+\alpha z)y^2}, \end{aligned}$$

where $h_1 > 0, h_2 > 0$ represents the handling time and h_3 represents how the handling time increases with prey density due to group defense. $p_1 > 0, p_2 > 0$ are the search rates of the predator toward susceptible and infected prey, respectively. $\alpha > 0$ is the parameter describing predator cooperation during hunting. We assume that juvenile prey cannot exhibit group defence against predators. The rate of prey consumption by a predator is considered to vary with prey density. Conversely, mature prey is presumed

to be capable of employing group defence mechanisms against predator attacks. Therefore, we utilize the functions $\phi_1(x,z)$ and $\phi_2(y,z)$ to represent the interactions between juvenile prey and predators and mature prey and predators, respectively. Thus model (2.4) becomes:

$$\begin{aligned}\frac{dx}{dt} &= \frac{ry}{1+f\alpha z} - bx(1-\delta x) - d_1 x - \phi_1(x,z),\\ \frac{dy}{dt} &= bx(1-\delta x) - d_2 y - \phi_2(y,z),\\ \frac{dz}{dt} &= c_1\phi_1(x,z) + c_2\phi_2(y,z) - d_3 z - nz^2,\end{aligned} \tag{2.5}$$

with the initial conditions $x(0) > 0$, $y(0) > 0$, $z(0) > 0$, where $c_1 > 0$, $c_2 > 0$ are the conversion coefficients.

3. Mathematical preliminaries

The positivity and boundedness of solutions in prey-predator models are crucial for preserving biological realism, validity, and applicability. The positivity of solutions guarantees an accurate representation of population sizes and correct modelling of ecosystem interactions and dynamics, enabling effective management and conservation strategies. In a real-world context, the predator and prey population sizes cannot grow or decline indefinitely without being subjected to ecological constraints and environmental factors that limit their growth and ensure that they remain within certain boundaries over time. Hence, it is necessary to analyze the boundedness of solutions in the proposed model to ensure that it appropriately captures the dynamics of these populations in natural environments. In the study of population dynamics, equilibrium points play a significant role. A stable equilibrium point represents sustainable levels of population sizes that can persist over time. In this section, we present the positivity and boundedness of the proposed system (2.5) and determine the existence of the possible biologically feasible equilibrium states.

3.1. Positivity

Theorem 3.1. System (2.5) is positively invariant.

Proof. Solving system (2.5) with positive initial conditions $(x(0), y(0), z(0))$, we obtain the following:

$$\begin{aligned}x(t) &= x(0)\exp\left\{\frac{ry}{x(1+f\alpha z)} - b(1-\delta x) - d_1 - \frac{\phi_1(x,z)}{x}\right\},\\ y(t) &= y(0)\exp\left\{\frac{bx(1-\delta x)}{y} - d_2 - \frac{\phi_2(y,z)}{y}\right\},\\ z(t) &= z(0)\exp\left\{\frac{c_1\phi_1(x,z)}{z} + \frac{c_2\phi_2(y,z)}{z} - d_3 - nz\right\}.\end{aligned}$$

From the above three equations, we conclude that any solution starting with positive initial conditions $(x(0), y(0), z(0))$ in the interior of $\mathbb{R}^+_3$ remains there for all future time. ∎

3.2. Boundedness

Theorem 3.2. The orbits of system (2.5) are uniformly bounded, i.e., there exists a bounded set $\mathcal{B}$ such that for every orbit $(x(t), y(t), z(t))$ of (2.5) there is a time t_0 such that $(x(t), y(t), z(t)) \in \mathcal{B}$ for all $t \geq t_0$.

Proof. Let us define a function $U(t) = \frac{c_1}{c_2}x(t) + y(t) + \frac{1}{c_2}z(t)$. Then

$$\frac{dU}{dt} = \frac{c_1}{c_2}\frac{dx}{dt} + \frac{dy}{dt} + \frac{1}{c_2}\frac{dz}{dt}.$$

Now choose any μ with $0 < \mu < \left(d_2 - \frac{rc_1}{c_2}\right)$. Then,

$$\begin{aligned}&\frac{dU}{dt} + \mu U\\ &\leq \left(\frac{c_1 r}{c_2}\right)y + \frac{c_1 b\delta}{c_2}x^2 - \frac{c_1}{c_2}d_1 x + bx - b\delta x^2 - d_2 y - \frac{d_3}{c_2}z\\ &- \frac{n}{c_2}z^2 + \mu\left(\frac{c_1}{c_2}x + y + \frac{z}{c_2}\right)\\ &= y\left(\mu - \left(d_2 - \frac{rc_1}{c_2}\right)\right) + x\left(b - \frac{c_1}{c_2}d_1 + \frac{\mu c_1}{c_2}\right) + x^2\left(\frac{c_1 b\delta}{c_2} - b\delta\right)\\ &+ z\left(\frac{\mu}{c_2} - \frac{d_3}{c_2}\right) - \frac{nz^2}{c_2}\\ &\leq a_0 x - a_1 x^2 + b_0 z - b_1 z^2\\ &\leq -a_1\left(x - \frac{a_0}{2a_1}\right)^2 + \frac{a_0^2}{4a_1} - b_1\left(z - \frac{b_0}{2b_1}\right)^2 + \frac{b_0^2}{4b_1}\\ &\leq \frac{a_0^2}{4a_1} + \frac{b_0^2}{4b_1}\end{aligned}$$

where $a_0 = \left(b - \frac{c_1}{c_2}d_1 + \frac{mc_1}{c_2}\right)$, $a_1 = \left(b\delta - \frac{c_1 b\delta}{c_2}\right)$, $b_0 = \left(\frac{\mu}{c_2} - \frac{d_3}{c_2}\right)$, $b_1 = \frac{n}{c_2}$.

Define $K = \frac{a_0^2}{4a_1} + \frac{b_0^2}{4b_1}$. Then the above differential inequality can be written in the form

$$\frac{d}{dt}\left(U - \frac{K}{\mu}\right) \leq -\mu\left(U - \frac{K}{\mu}\right).$$

Now, by applying Lemma 2 on page 27 in Birkhoff and Rota (1989) [44], we obtain

$$0 \leq U(t) \leq \frac{K}{\mu}\left(1 - e^{-\mu t}\right) + U(0)e^{-\mu t}.$$

For any $\epsilon > 0$, define

$$\mathcal{B} = \left\{(x, y, z) : x \geq 0, y \geq 0, z \geq 0, \frac{c_1}{c_2}x + y + \frac{1}{c_2}z \leq \frac{K}{\mu} + \epsilon\right\}.$$

Then, for every orbit of (2.5), there is a time t_0 such that $(x(t), y(t), z(t)) \in \mathcal{B}$ for all $t \geq t_0$. ■

3.3. Equilibrium points

An equilibrium point is a type of solution of a system that does not change with time. From an ecological viewpoint, it is a state where all the species achieve a fixed population irrespective of the initial population. In ecological systems, equilibrium points are determined by comparing the rates of change of all species' populations to zero. Our proposed system (2.5) has three ecologically feasible equilibrium points: the trivial equilibrium (E_0), the predator-free equilibrium (E_1), and the interior equilibrium (E^*). The trivial or the zero equilibrium, $E_0(0, 0, 0)$, always exists. The predator-free equilibrium, $E_1(\bar{x}, \bar{y}, 0)$, where $\bar{x} = \frac{br - d_2(b+d_1)}{b\delta(r-d_2)}$, $\bar{y} = \frac{d_1(br - d_2(b+d_1))}{b\delta(r-d_2)^2}$, exists whenever the maximum per capita growth rate of the matured prey (r) is greater than the natural mortality of the matured prey (d_2) as well as the threshold value $\frac{d_2(b+d_1)}{b}$, i.e., $r > \min\left\{d_2, \frac{(b+d_1)d_2}{b}\right\}$. The other non-trivial equilibrium is the interior equilibrium $E^*(x^*, y^*, z^*)$ where $x^* \neq 0$, $y^* \neq 0$, and $z^* \neq 0$.

Suppose $z^* \neq 0$. The juvenile prey nullcline gives

$$\begin{aligned} y^* = {} & \frac{1}{r}(1 + \alpha f z^*) \\ & \times \left(bx^*(1 - \delta x^*) + d_1 x^* \right. \\ & \left. + \frac{x^* z^* \left(p_1 + \alpha z^*\right)}{1 + h_1 x^* \left(p_1 + \alpha z^*\right)}\right) > 0. \end{aligned} \tag{3.1}$$

The predator nullcline gives

$$x^* = \frac{A_0 - (A_2 + 1)\, d_3 - n z^*}{(p_1 + \alpha z^*)\left(h_1\left((A_2 + 1)\, d_3 + n z^* - A_0\right) - A_1\right)}, \tag{3.2}$$

where

$$\begin{aligned} A_0 &= y^*\left(p_2 + \alpha z^*\right)\left(c_2 - n z^*\left(h_3 y^* + h_2\right)\right), \\ A_1 &= c_1\left(y^*\left(h_3 y^* + h_2\right)\left(p_2 + \alpha z^*\right) + 1\right), \\ A_2 &= y^*\left(h_3 y^* + h_2\right)\left(p_2 + \alpha z^*\right). \end{aligned}$$

$A_0 > 0$ if $c_2 - n z^*\left(h_3 y^* + h_2\right) > 0$.

$x^* > 0$ either if

(a) $A_0 - (A_2 + 1)\, d_3 - n z^* > 0$,
$h_1\left(n z^* + (A_2 + 1)\, d_3 - A_0\right) - A_1 > 0$.

(b) $A_0 - (A_2 + 1)\, d_3 - n z^* < 0$,
$h_1\left(n z^* + (A_2 + 1)\, d_3 - A_0\right) - A_1 < 0$.

For the parameters provided in Table 1, the numerically obtained solution of the system is $(0.3226, 0.1688, 0.5540)$. Solving (3.2) and (3.1), using parameters in Table 1 and $z^* = 0.5540$, gives $x^* = 0.3226$ and $y^* = 0.1688$, respectively, and condition (b) holds.

Table 1. Parameter values. Parameters are considered in *per unit time.*

Parameter	Default value
Birth rate in prey (r)	1
Density factor (δ)	0.1
Predation rate (p_1)	0.3
Predation rate (p_2)	0.4
Conversion rate (b)	0.2
Conversion of energy (c_1)	0.8
Conversion of energy (c_2)	0.7
Death rate in juvenile prey (d_1)	0.1
Death rate in matured prey (d_2)	0.1
Death rate in predator (d_3)	0.1
Hunting cooperation rate (α)	0.2
Handling time (h_1)	0.5
Handling time (h_2)	0.5
Handling time (h_3)	0.5
Fear parameters for Juvenile's growth (f)	0.3
Intraspecies competition among predators (n)	0.1

4. Local stability analysis

In this section, we discuss the local stability of the system near the equilibrium states. We utilize the Hartmann-Grobmann theorem and Routh-Hurwitz criteria throughout this discussion. The Jacobian of system (2.5) is given by

$$J = \begin{pmatrix} J_{11} & J_{12} & J_{13} \\ J_{21} & J_{22} & J_{23} \\ J_{31} & J_{32} & J_{33} \end{pmatrix}, \tag{4.1}$$

where

$$\begin{aligned}
J_{11} &= b(2\delta x - 1) - d_1 - \frac{z\,(p_1 + \alpha z)}{(h_1 x\,(p_1 + \alpha z) + 1)^{\,2}}, \\
J_{12} &= \frac{r}{\alpha f z + 1}, \\
J_{13} &= -\frac{\alpha f r y}{(\alpha f z + 1)^2} - \frac{x\left(h_1 x\,(p_1 + \alpha z)^{\,2} + p_1 + 2\alpha z\right)}{(h_1 x\,(p_1 + \alpha z) + 1)^{\,2}}, \\
J_{21} &= b - 2b\delta x, \\
J_{22} &= \frac{z\,(p_2 + \alpha z)\left(h_3 y^2\,(p_2 + \alpha z) - 1\right)}{(y\,(h_3 y + h_2)\,(p_2 + \alpha z) + 1)^{\,2}} - d_2, \\
J_{23} &= \frac{y\left(-y\,(h_3 y + h_2)\,(p_2 + \alpha z)^{\,2} - p_2 - 2\alpha z\right)}{(y\,(h_3 y + h_2)\,(p_2 + \alpha z) + 1)^{\,2}}, \\
J_{31} &= \frac{c_1 z\,(p_1 + \alpha z)}{(h_1 x\,(p_1 + \alpha z) + 1)^{\,2}}, \\
J_{32} &= -\frac{c_2 z\,(p_2 + \alpha z)\left(h_3 y^2\,(p_2 + \alpha z) - 1\right)}{(y\,(h_3 y + h_2)\,(p_2 + \alpha z) + 1)^{\,2}}, \\
J_{33} &= \frac{c_1 x\left(h_1 x\,(p_1 + \alpha z)^{\,2} + p_1 + 2\alpha z\right)}{(h_1 x\,(p_1 + \alpha z) + 1)^{\,2}} \\
&\quad + \frac{c_2 y\left(y\,(h_3 y + h_2)\,(p_2 + \alpha z)^{\,2} + p_2 + 2\alpha z\right)}{(y\,(h_3 y + h_2)\,(p_2 + \alpha z) + 1)^{\,2}} - d_3 - 2nz.
\end{aligned}$$

4.1. Local stability at E_0

The eigenvalues of the Jacobian matrix (4.1) at the trivial equilibrium E_0 are

$$\begin{aligned}
\lambda_1 &= -d_3 < 0, \\
\lambda_{2,3} &= \frac{1}{2}\Big(- b - d_1 - d_2 \\
&\quad \pm \sqrt{(b + d_1 + d_2)^{\,2} - 4\,(bd_2 - br + d_1 d_2)}\Big).
\end{aligned}$$

- If $(b + d_1 + d_2)^{\,2} - 4\,(bd_2 - br + d_1 d_2) < 0$, the system will have a pair of imaginary eigenvalues. Since the real parts of $\lambda_{1,2,3}$ are negative, the trivial equilibrium E_0 will be locally asymptotically stable.
- If $(b + d_1 + d_2)^{\,2} - 4\,(bd_2 - br + d_1 d_2) > 0$, the trivial equilibrium E_0 will be locally asymptotically stable if

$$\sqrt{(b + d_1 + d_2)^{\,2} - 4\,(bd_2 - br + d_1 d_2)} < b + d_1 + d_2.$$

4.2. Local stability at E_1

Due to the complexity of the proposed model, we utilize the Routh-Hurwitz criteria to analyze the local stability at E_1. The characteristic equation of the Jacobian matrix (4.1) at the predator-free equilibrium E_1 has the form

$$\rho^3 + D_1\rho^2 + D_2\rho + D_3 = 0, \tag{4.2}$$

where D_i are functions of the state variables $\bar{x}$, $\bar{y}$, $\bar{z}$.

$$\begin{aligned}
D_1 &= b(1 - 2\delta\bar{x}) + d_1 + d_2 + (d_3 - \varrho), \\
D_2 &= b(-1 + 2\delta\bar{x})\,(d_2 + d_3 + r) + d_1 d_2 + d_1 d_3 + d_2 d_3 \\
&\quad + (b(2\delta\bar{x} - 1) - d_1 - d_2)\varrho, \\
D_3 &= (d_2\,(b - 2b\delta\bar{x} + d_1) - br(1 - 2\delta\bar{x}))(d_3 - \varrho), \\
\varrho &= \left(\frac{c_1 p_1 \bar{x}}{h_1 p_1 \bar{x} + 1} + \frac{c_2 p_2 \bar{y}}{h_3 p_2 \bar{y}^2 + h_2 p_2 \bar{y} + 1}\right).
\end{aligned}$$

Whenever $r > \min\left\{d_2, \frac{(b+d_1)d_2}{b}\right\}$, $\varrho > 0$.
$D_1 > 0$ if $\bar{x} < \frac{1}{2\delta}$ and $d_3 > \varrho$.
$D_2 > 0$ if $\bar{x} < \frac{1}{2\delta}$, $d_3 > \varrho$, and
$d_1 d_2 + d_3 d_2 + d_1 d_3 > b(1-2\delta x)\,(\varrho + d_2 + d_3 + r) + \varrho\,(d_1 + d_2)$.
$D_3 > 0$ if $\bar{x} < \frac{1}{2\delta}$, $d_3 > \varrho$, and $d_1 d_2 > b\,(r - d_2)\,(1 - 2\delta\bar{x})$.

By the Routh-Hurwitz criteria, the predator-free equilibrium E_1 is locally asymptotically stable if $D_1, D_3 > 0$ and $\Delta = D_1 D_2 - D_3 > 0$, and E_1 experiences a Hopf bifurcation for some free parameter f (say) at a threshold value $f = f^H$ if $D_1(f^H), D_3(f^H) > 0$, $\Delta = D_1(f^H)D_2(f^H) - D_3(f^H) = 0$, and $\frac{\partial\Delta}{\partial f}(f^H) \neq 0$.
Remark: Please note that expressing D_i $(i = 1, 2, 3)$ explicitly in terms of $\bar{x}$ and $\bar{y}$ results in very lengthy and complex formulas. Therefore, we have chosen to avoid these explicit expressions in this paper.

4.3. Local stability at E^*

The characteristic equation of the Jacobian matrix (4.1) at the interior equilibrium E^* has the form

$$\rho^3 + B_1\rho^2 + B_2\rho + B_3 = 0, \tag{4.3}$$

where B_i are functions of the state variables x^*, y^*, z^*.

$$
\begin{aligned}
B_1 &= b(1-2\delta x^*) + d_1 + d_2 + (d_3 - \varrho),\\
B_2 &= b(-1+2\delta x^*)(d_2+d_3+r) + d_1d_2 + d_1d_3 + d_2d_3\\
&\quad + (b(2\delta x^* - 1) - d_1 - d_2)\varrho,\\
B_3 &= (d_2(b - 2b\delta x^* + d_1) - br(1-2\delta x^*))(d_3 - \varrho),\\
\varrho &= \left(\frac{c_1p_1x^*}{h_1p_1x^* + 1} + \frac{c_2p_2y^*}{h_3p_2y^{*2} + h_2p_2y^* + 1}\right).
\end{aligned}
$$

By the Routh-Hurwitz criteria, the interior equilibrium E^* is locally asymptotically stable if $B_1, B_3 > 0$ and $\Delta = B_1B_2 - B_3 > 0$, and E^* experiences a Hopf bifurcation for some free parameter f (say) at a threshold value $f = f^H$ if $B_1(f^H), B_3(f^H) > 0$, $\Delta = B_1(f^H)B_2(f^H) - B_3(f^H) = 0$, and $\frac{\partial\Delta}{\partial f}(f^H) \neq 0$.

Remark: Note that the determination of B_i $(i = 1, 2, 3)$ explicitly in terms of x^*, y^*, and z^* is not possible due to the complexity of the model.

5. Bifurcation analysis

Theorem 5.1. System (2.5) at the predator-free equilibrium E_1 undergoes a transcritical bifurcation when parameter b passes through critical parameter value $b = b^{TC}$, where neither a saddle-node bifurcation nor a pitchfork bifurcation can occur.

Proof. The Jacobian matrix of system (2.5) at the predator-free equilibrium E_1 has an eigenvalue of zero at the critical parameter $b = b^{TC}$. The critical value b^{TC} is a solution of the following polynomial equation:

$$
\begin{aligned}
&\Big(\psi_1(d_1p_2(\psi_1p_1\left(\psi_1c_1d_1h_3 + b\psi_2^2\delta\left(c_2h_1 + c_1h_2\right)\right) + b^2\psi_2^3c_2\delta^2)\\
&+ b^2\psi_2^4c_1\delta^2p_1)\Big)/\Big((\psi_1h_1p_1 + b\psi_2\delta)(\psi_1d_1p_2(\psi_1d_1h_3\\
&+ b\psi_2^2\delta h_2) + b^2\psi_2^4\delta^2)\Big) = 0,
\end{aligned}
$$

where $\psi_1 = br - d_2(b + d_1)$, $\psi_2 = r - d_2$.

So the eigenvalue analysis method fails to predict the nature of the equilibrium point at the critical value $b = b^{TC}$. Therefore we use Sotomayor's theorem [45] to investigate the nature of the equilibrium E_1 at $b = b^{TC}$. Rewrite system (2.5) as follows:

$$
\frac{dX}{dt} = \tilde{g}(X, b) = [g_1(X, b), g_2(X, b), g_3(X, b)]^T,
$$

where $X = \begin{pmatrix} x \\ y \\ z \end{pmatrix}$, $g_1(X, b) = \frac{dx}{dt}$, $g_2(X, b) = \frac{dy}{dt}$, and $g_3(X, b) = \frac{dz}{dt}$.

Let $V = [v_1, v_2, v_3]^T$ and $W = [0, 0, 1]^T$ be, respectively, the eigenvectors of J_{E_1} and $[J_{E_1}]^T$ corresponding to the zero eigenvalue at $b = b^{TC}$. Then we have

$$
\begin{aligned}
W^T\tilde{g}_b(X, b^{TC})_{E_1} &= 0,\\
W^TD\tilde{g}_b(X, b^{TC})(V)_{E_1} &\neq 0.
\end{aligned}
\tag{5.1}
$$

Therefore, the first two conditions of the transcritical bifurcation are met, whilst saddle-node and pitchfork bifurcation cannot occur. Now

$$
\begin{aligned}
&D^2\tilde{g}(X, b^{TC})_{E_1}\\
&= \begin{pmatrix}
2\delta b^{\mathrm{TC}} & 0 & -\frac{p_1}{(h_1p_1\bar{x}+1)^2}\\
0 & 0 & \frac{p_2\left(h_3p_2\bar{y}^2-1\right)}{\left(h_3p_2\bar{y}^2+h_2p_2\bar{y}+1\right)^2}\\
\frac{c_1p_1}{(h_1p_1\bar{x}+1)^2} & -\frac{c_2p_2\left(h_3p_2\bar{y}^2-1\right)}{\left(h_3p_2\bar{y}^2+h_2p_2\bar{y}+1\right)^2} & \chi_0
\end{pmatrix},
\end{aligned}
$$

where

$$
\chi_0 = \frac{2\alpha c_1\bar{x}}{(h_1p_1\bar{x}+1)^2} + \frac{2\alpha c_2\bar{y}}{(h_3p_2\bar{y}^2 + h_2p_2\bar{y} + 1)^2} - 2n.
$$

Therefore

$$
\begin{aligned}
&W^TD^2\tilde{g}(X, b^{TC})(V, V)_{E_1}\\
&= v_3\Big(\frac{c_1(p_1v_1 + 2\alpha v_3\bar{x})}{(h_1p_1\bar{x}+1)^2} +\\
&\frac{c_2\left(p_2v_2 + 2\alpha v_3\bar{y} - h_3p_2^2v_2\bar{y}^2\right)}{(h_3p_2\bar{y}^2 + h_2p_2\bar{y} + 1)^2} - 2nv_3\Big) \neq 0.
\end{aligned}
$$

Thus, the system satisfies all the conditions of Sotomayor's theorem for transcritical bifurcation. Therefore, system (2.5) undergoes a transcritical bifurcation at the parameter $b = b^{TC}$ at the predator-free equilibrium E_1.

■

6. Numerical simulations

In this section, we perform numerical simulations of solutions of system (2.5) using the parameter set given in Table 1. For the above parameters, the trajectory of system (2.5), with initial population $x = 0.1$, $y = 0.5$,

and $z = 0.8$, converges to a stable interior equilibrium $E^*(0.3226, 0.1688, 0.5540)$. In Figure 1, we plot the time series solution of the interior equilibrium with $t = 3000$ units. Each population initially starts oscillating and approaches E^*. Considering this interior equilibrium E^*, in the next sections, we discuss the effects of some of the significant parameters on the system dynamics.

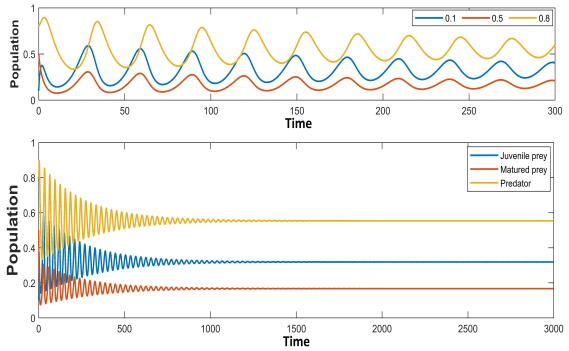

Figure 1. Time series solution of system (2.5) for $t = 3000$ with the initial value $(0.1, 0.5, 0.8)$. All the parameters are taken from Table 1.

6.1. *Effect of hunting cooperation rate α*

Starting from the interior equilibrium E^*, we compute the curve of interior equilibrium with the free parameter α, using the MATLAB-based continuation software package MatCont 7.3 [46]. For increasing values of the hunting cooperation rate α, the interior equilibrium E^* undergoes a Hopf bifurcation at $\alpha = \alpha^H \approx 0.256590$. The first Lyapunov coefficient at the Hopf bifurcation point $\alpha = \alpha^H$ is found to be $l_1 = 3.708334 \times 10^{-03}$, which suggests the nature of the Hopf to be subcritical. Due to supercritical Hopf bifurcation, unstable periodic solutions emerge for $\alpha > \alpha^H$. Initiating from the Hopf point $\alpha = \alpha^H$, we plot the periodic orbits with the same parameter α, which leads to stable periodic solutions followed by saddle-node bifurcation of limit cycles (denoted as LPC) at $\alpha^{LPC} \approx 0.2565918$. At the bifurcation point α^{LPC}, the periodic solutions emerging due to the Hopf bifurcation gain stability and form stable periodic solutions for $\alpha > \alpha^{LPC}$. Figure 2 describes the graphical representation of the scenario of periodic solutions due to the said bifurcation. Initiating from the Hopf point $\alpha = \alpha^H$, we plot the two-dimensional projection of the Hopf bifurcation curve for the parameter spaces (α, f) and (α, n). Figure 3 represents the region where two interior equilibrium E^* of different stabilities can be observed. The space above the Hopf curve in Figure 3 represents the region where interior equilibria are stable while the space below the Hopf curve represents the region where interior equilibria are unstable.

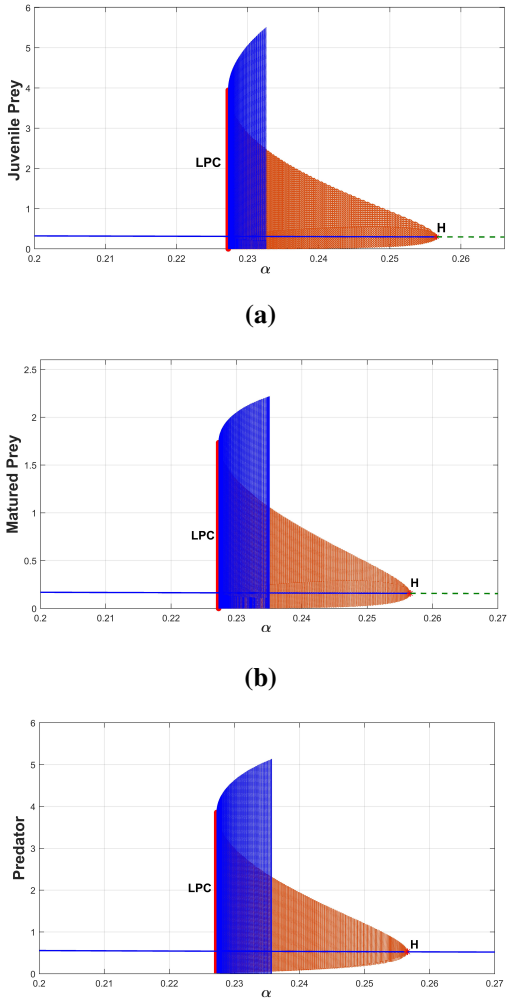

(a)

(b)

(c)

Figure 2. Periodic solutions via Hopf bifurcation with respect to the parameter α. Other parameters are taken from Table 1.

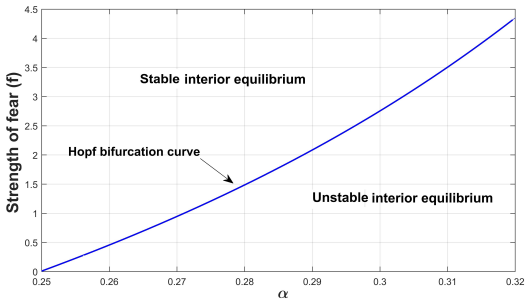

Figure 3. Two-dimensional projection of the Hopf bifurcation curve with respect to α and f. Other parameters are taken from Table 1.

A similar two-dimensional projection of the Hopf bifurcation curve is plotted for varying parameters α and n (Figure 4). The plotted Hopf curve undergoes a generalized-Hopf bifurcation at the point $GH = (\alpha \approx 1.481421, n \approx 0.470238)$. At this point, GH, the first Lyapunov coefficient becomes zero and the periodic solutions exchange their nature from subcritical to supercritical. At GH, the second Lyapunov coefficient is found to be $l_2 = 7.907562 \times 10^{-03}$.

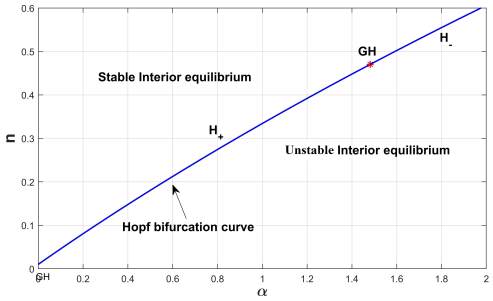

Figure 4. Two-dimensional projection of the Hopf bifurcation curve with respect to α and n. Other parameters are taken from Table 1.

6.2. *Effect of conversion rate b*

Starting from the interior equilibrium E^*, we compute the curve of the interior equilibrium with the conversion rate b as a free parameter. For decreasing values of b, the interior equilibrium E^* undergoes a transcritical bifurcation at $b = b^{TC} \approx 0.011568$, with state space $(0.3948460.043872, 0)$.

For increasing values of the conversion rate b, the interior equilibrium E^* undergoes another subcritical Hopf at $b = b^H \approx 0.455130$, where the first Lyapunov coefficient is $l_1 = 9.889108 \times 10^{-03}$. In Figure 5, initiating from the Hopf point $b = b^H$, the two-dimensional projection of the Hopf bifurcation curve is plotted for varying parameters b and p_1. This leads to another generalized-Hopf bifurcation at $GH = (b \approx 0.126613, p_1 \approx 0.174932)$. Above the Hopf curve, the interior equilibrium is stable, and it is unstable in the region below the curve.

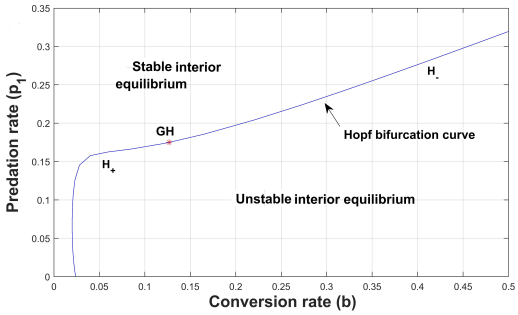

Figure 5. Two-dimensional projection of the Hopf bifurcation curve with respect to b and p_1. Other parameters are taken from Table 1.

To analyze the effect of the density factor and conversion rate on the proposed ecosystem, we conduct simulations with free parameters δ and b, initiating from the Hopf point $b = b^H$ and transcritical bifurcation point $b = b^{TC}$. We plot the Hopf curve and saddle-node curve initiating from $b = b^H$ and $b = b^{TC}$ in the parametric space (δ, b), as shown in Figure 6. The Hopf bifurcation curve leads to a generalized-Hopf bifurcation at $GH(\delta \approx 0.510059, b \approx 0.983975)$ and the saddle-node bifurcation leads to a Bogdanov-Takens bifurcation at $BT(\delta \approx 0.011112, b \approx 0.000105)$.

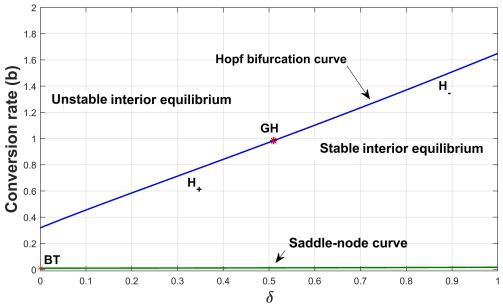

Figure 6. Two-dimensional projection of the Hopf bifurcation curve with respect to δ and b. Other parameters are taken from Table 1.

6.3. *Effect of predation rates p_1 and p_2*

To analyze the effect of predation on the proposed ecosystem, we conduct simulations with free parameters p_1 and p_2, initiating from the Hopf point obtained at $p_1 = p^H \approx 0.196997$ by the continuation of the internal equilibria curve E^*. Figure 7 describes the region separated by the Hopf curve, where internal equilibria of different stabilities can be observed.

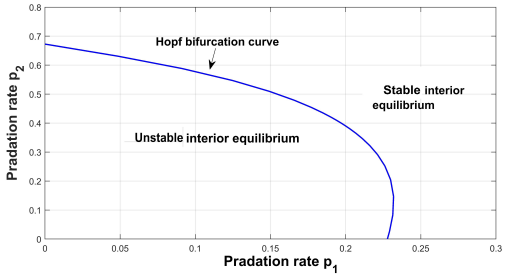

Figure 7. Two-dimensional projection of the Hopf bifurcation curve with respect to p_1 and p_2. Other parameters are taken from Table 1.

6.4. *Effect of the death rate of predators d_3*

Initiating from the interior equilibrium point E^*, taking d_3 as a free parameter, the curve of interior equilibrium is computed in Figure 8. This leads to the detection of two Hopf bifurcation points at $H_1 \approx 0.124697$ and $H_2 \approx 1.048329$, respectively. At the Hopf point, the nature of the Hopf bifurcation is subcritical ($l_1 = 3.412286 \times 10^{-03}$), which later undergoes a saddle-node bifurcation of limit cycles at $LPC \approx 0.112868$, thereby gaining stability of the periodic orbits that emerged at H_1. These periodic orbits again undergo two period-doubling bifurcations at $PD_1 \approx 0.2736144$ and $PD_2 \approx 1.002934$, followed by a transcritical bifurcation of limit cycles at $BPC \approx 1.048329$ (Figure 9). In our case, the Hopf point H_2 coincides with the BPC. Again, as the system progresses, the periodic orbits emerging from the initial period-doubling point, PD_1, exhibit a fascinating phenomenon. They undergo multiple period-doubling bifurcations at distinct thresholds: $PD_3 \approx 0.8220511$, $PD_4 \approx 0.8578651$, $PD_5 \approx 0.8835957$, and $PD_6 \approx 0.941419$. These bifurcations signify a complex pattern of transition within the system's dynamics. In Figure 10, these transformations are visually depicted, offering insight into the complex behavior of the system. Furthermore, Figure 11 provides a comprehensive overview, capturing the entirety of the observed period-doubling bifurcation phenomena for the bifurcation parameter d_3, thus contributing to a deeper understanding of the system's dynamics and its underlying complexities. In population models, period doubling can occur, which replicates a scenario where the population exhibits regular, periodic oscillations in abundance.

Understanding these dynamics is crucial for predicting population sizes and their environmental interactions. In stage-structured models, interactions between age classes or stages, as well as environmental factors, frequently result in period doubling. Period doubling can provide insight into how stage-specific feedback mechanisms help populations self-regulate throughout time. For example, oscillations in predator and prey populations may have a period-doubling pattern in a predator-prey model with stage structure, where predators alternate between targeting various stages of prey depending on their abundance. Period doubling in stage-structured models can reflect the optimization of life history strategies in response to environmental variability. For example, organisms may adjust their reproductive effort or allocation to growth in response to changes in resource availability or predation pressure, leading to oscillations in population dynamics. In our case, it can be thought that whenever the mortality rate of predators increases and crosses a certain critical threshold, the prey population might experience a release from predation pressure, leading to an increase in their numbers. This initial increase can lead to a period-doubling cascade. Beyond a certain point, further increases in predator mortality might stabilize the system again. This could be due to various reasons, such as changes in resource competition, shifts in reproductive strategies, or the introduction of new ecological interactions. When these additional factors come into play, they can reduce the oscillations, leading to an equilibrium state where the populations of both prey and predators coexist in a stable manner.

We plot the phase portraits of the system (2.5) for different values of the bifurcation parameter d_3 in Figure 12. Furthermore, although between the points H_1 and H_2, the predator population shows an oscillatory nature, for $d_3 \in (0, M \approx 0.760755]$, the overall population of predators

increases. This clearly indicates the existence of a positive Hydra effect in the predator population.

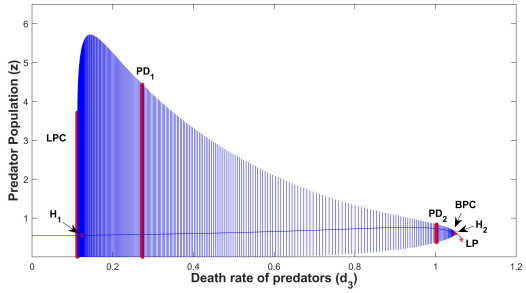

Figure 8. Period-doubling bifurcation points PD_1 and PD_2 with respect to d_3. Other parameters are taken from Table 1.

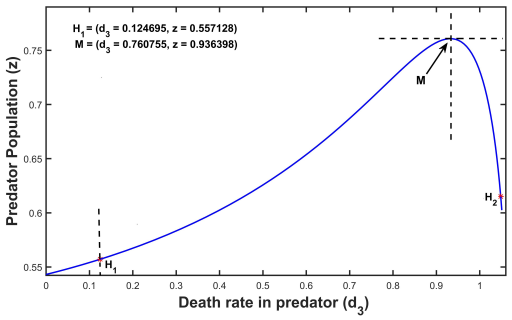

Figure 9. Depicts stable stocks for all the predator population when d_3 increases. Biomass of the predator population is increased for $d_3 \in (0, M \approx 0.760755]$, confirming the existence of the hydra effect.

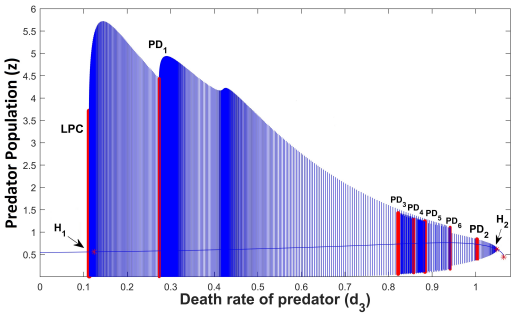

Figure 10. Multple period-doubling bifurcations with respect to d_3. Other parameters are taken from Table 1.

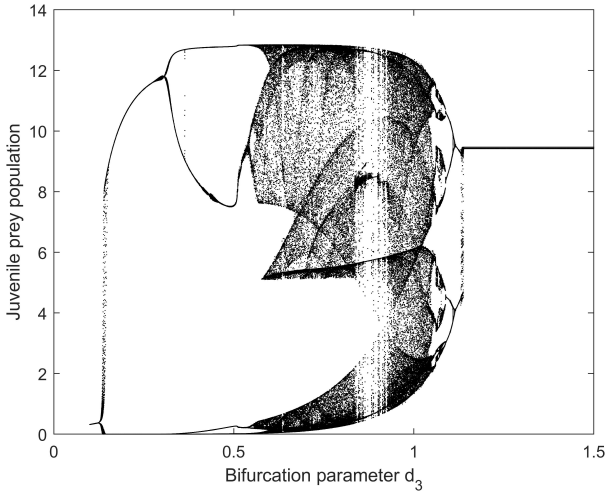

(a)

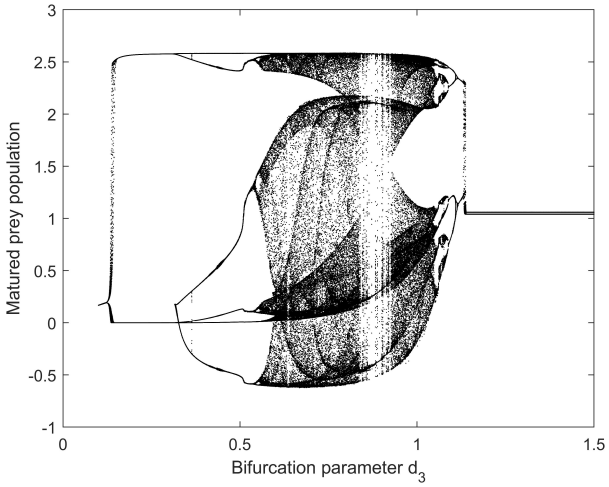

(b)

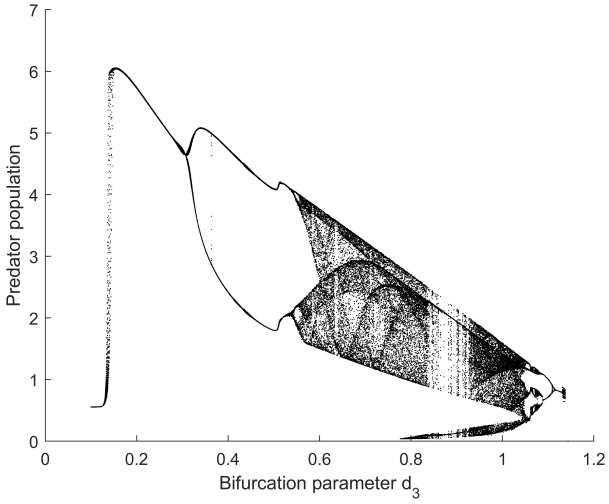

(c)

Figure 11. Bifurcation diagram with respect to bifurcation parameter d_3. Other parameters are taken from Table 1.

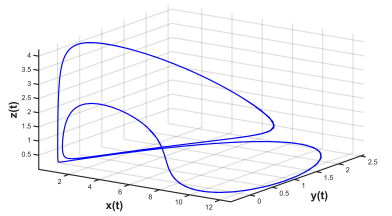

(a)

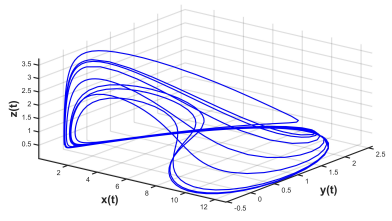

(b)

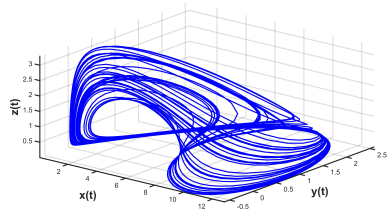

(c)

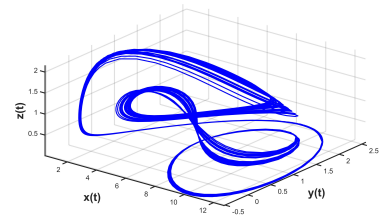

(d)

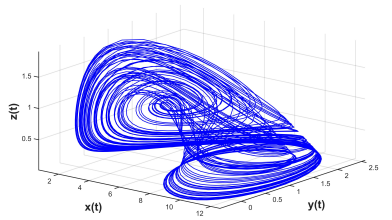

(e)

Figure 12. Phase portrait of system (2.5) for (a) $d_3 = 0.4$, (b) $d_3 = 0.52$, (c) $d_3 = 0.6$, (d) $d_3 = 0.8$, and (e) $d_3 = 0.84$. Other parameters are taken from Table 1.

7. Conclusions and future scopes

Throughout this work, we proposed and analyzed a complex mathematical model considering a stage-structured predator-prey system. Stage-structured compartments are assumed for the prey population. The psychological phenomenon of the cost of fear due to the predation process and its combined increased rate due to hunting cooperation was analyzed. The positiveness and boundedness of solutions of the proposed system were analyzed with the help of Gronnwall's inequality. The dynamics of the model were discussed near the possible steady states of the system. Theories of the bifurcation analysis were used to estimate the threshold values of parameters at which qualitative changes occur in the proposed system, such as the appearance or disappearance of periodic behavior and the emergence of a new equilibrium. For a certain set of parameters, the proposed system (2.5) has an interior equilibrium state where all species populations coexist. The system under consideration also demonstrates a state of equilibrium where predators are absent. Depending on the specific threshold parameter values, the system can shift into a predator-free state. In a system where all species coexist, if the level of cooperation in hunting among them surpasses a certain threshold, it leads to instability and causes the populations of the species to fluctuate periodically. However, the periodic oscillations resulting from this instability are not initially stable. They gain stability through a phenomenon called saddle-node bifurcation limit cycles, eventually leading to the formation of stable periodic oscillations in the populations of the species. There is a strong correlation between hunting cooperation and two other parameters: the level of fear among the species and the extent of intraspecies competition. A higher rate of hunting cooperation has a more significant impact on the reproduction rate of prey and also intensifies the intraspecies competition among predators. According to our computational findings, if the levels of hunting cooperation and intra-species competition rates exceed a certain threshold, the populations of the species will commence periodic oscillations. In our proposed system, the process of juvenile prey transitioning into mature individuals is an essential factor that must

be considered. This conversion rate holds significant importance to the overall dynamics of the system. When the conversion rate falls below a certain threshold value, the ecosystem becomes devoid of predators, and when it exceeds a certain threshold value, the system becomes unstable, resulting in periodic population oscillations.

The predation rate on juvenile prey and the conversion rate are strongly correlated, as a higher predation rate results in a slower conversion rate. This correlation can be attributed to the impact of fear caused by the predation process, which is often observed during the conversion process. In other words, the cost of fear associated with predation can affect the conversion process. Although we did not explicitly consider the conversion function to be impacted by the cost of fear, the discussion on these two interrelated factors is significant. Once the predation rate on juvenile prey and the conversion rate surpass a certain threshold value, the coexistence equilibrium state of the ecosystem becomes unstable, leading to periodic oscillations of the population densities. The density factor of the logistic growth is another factor that strongly correlates with the conversion rate. Our computational results show periodic oscillation of the species populations when the density factor and conversion rate values exceed a threshold value. The predation process is a fundamental biological process that exerts a significant influence on the dynamics of populations, the structure of communities, and the functioning of ecosystems. The predators in our proposed system obtain advantages by preying on both juvenile and mature prey at distinct rates. As a result, it is crucial to discuss the overall impact of the predation process on the dynamics of the system. Numerically, we estimated a critical region in which the species populations show oscillatory behavior. Apart from its negative implications on mortality, the mortality rate could also stimulate a positive effect within the predator population. Once the mortality rate of predators crosses a specific threshold, it is notable that despite experiencing periodic oscillations, the predator population shows a gradual increase.

While numerous models have been developed to account for antipredator behaviors and cooperative hunting among predators, most of these models are situated within the framework of eco-epidemiological models. Roy et al. [35] investigated an eco-epidemic model with prey refuge by considering the cost of fear affecting reproduction and disease transmission. The predators are assumed to follow a cooperative hunting strategy during predation. Their study showed that the cost of fear causing a reduction in the birth rate of susceptible prey has a destabilizing role. In their research, Biswas et al. [36] studied how fear affects the dynamics of an eco-epidemiological switching model. Their findings showed that the force of infection and the fear factor, which affects the reproduction of prey, both destabilize the system's dynamics. In the context of stage structure, Panday et al. [32] showed that the absence of anti-predator behavior, combined with an increase in the maturation rate, could potentially lead to the extinction of all species in the system. Although different models have been carried out to study the role of antipredator behaviors and predator-prey dynamics, few works have been addressed in the context of stage structures. This becomes a significant gap in the study of predator-prey dynamics, and our present study offers a novel contribution to the said domain. It is important to note that our study relied solely on hypothetical data, and future research utilizing real-world data may yield more meaningful and applicable results. Future researchers may build upon our proposed model by examining the impact of the fear of predation risk on conversion rates. Additionally, exploring the potential for analyzing our model using fractional-ordered derivatives presents a promising opportunity for investigating more intricate and dynamic behavior.

Author contributions

All authors contributed equally and significantly in writing this paper. All authors read and approved the final manuscript.

Use of Generative-AI tools declaration

The authors declare that they have not used Artificial Intelligence (AI) tools in the creation of this article.

Acknowledgments

The authors sincerely thank the anonymous reviewers and the editorial team for their insightful comments and constructive feedback, which significantly enhanced the clarity, depth, and overall quality of this work.

Conflict of interest

The authors declare that there is no conflict of interest regarding the publication of this paper.

References

1. B. Ghosh, O. L. Zhdanova, B. Barman, E. Y. Frisman, Dynamics of stage-structure predator-prey systems under density-dependent effect and mortality, *Ecol. Complex.*, **41** (2020), 100812. https://doi.org/10.1016/j.ecocom.2020.100812
2. S. K. Sasmal, Y. Takeuchi, Dynamics of a predator-prey system with fear and group defence, *J. Math. Anal. Appl.*, **481** (2020), 123471. https://doi.org/10.1016/j.jmaa.2019.123471
3. S. Pal, N. Pal, S. Samanta, J. Chattopadhyay, Effect of hunting cooperation and fear in a predator-prey model, *Ecol. Complex.*, **39** (2019), 100770. https://doi.org/10.1016/j.ecocom.2019.100770
4. S. Creel, D. Christianson, S. Liley, J. A. Winnie, Predation risk affects reproductive physiology and demography of elk, *Science*, **315** (2007), 960–960. https://doi.org/10.1126/science.1135918
5. S. D. Peacor, B. L. Peckarsky, G. C. Trussell, J. R. Vonesh, Costs of predator-induced phenotypic plasticity: a graphical model for predicting the contribution of nonconsumptive and consumptive effects of predators on prey, *Oecologia*, **171** (2013), 1–10. https://doi.org/10.1007/s00442-012-2394-9
6. N. Mondal, D. Barman, S. Alam, Impact of adult predator incited fear in a stage-structured prey-predator model, *Environ. Dev. Sustain.*, **23** (2021), 9280–9307. https://doi.org/10.1007/s10668-020-01024-1
7. M. Das, G. P. Samanta, A prey-predator fractional order model with fear effect and group defence, *Int. J. Dyn. Control*, **9** (2021), 334–349. https://doi.org/10.1007/s40435-020-00626-x
8. L. Y. Zanette, A. F. White, M. C. Allen, M. Clinchy, Perceived predation risk reduces the number of offspring songbirds produce per year, *Science*, **334** (2011), 1398–1401. https://doi.org/10.1126/science.1210908
9. K. H. Elliott, G. S. Betini, I. Dworkin, D. R. Norris, Experimental evidence for within- and cross-seasonal effects of fear on survival and reproduction, *J. Anim. Ecol.*, **85** (2016), 507–515. https://doi.org/10.1111/1365-2656.12487
10. X. Wang, L. Zanette, X. Zou, Modelling the fear effect in predator–prey interactions, *J. Math. Biol.*, **73** (2016), 1179–1204. https://doi.org/10.1007/s00285-016-0989-1
11. C. Feh, T. Boldsukh, C. Tourenq, Are family groups in equids a response to cooperative hunting by predators? The case of Mongolian kulans (Equus hemionus luteus Matschie), *Revue D'écologie*, **49** (1994), 11–20. https://doi.org/10.3406/revec.1994.2123
12. P. A. Schmidt, L. D. Mech, Wolf pack size and food acquisition, *Am. Nat.*, **150** (1997), 513–517. https://doi.org/10.1086/286079
13. W. J. Ripple, E. J. Larsen, Historic aspen recruitment, elk, and wolves in northern Yellowstone National Park, USA, *Biol. Conserv.*, **95** (2000), 361–370. https://doi.org/10.1016/S0006-3207(00)00014-8
14. S. Creel, J. Winnie Jr, B. Maxwell, K. Hamlin, M. Creel, Elk alter habitat selection as an antipredator response to wolves, *Ecology*, **86** (2005), 3387–3397. https://doi.org/10.1890/05-0032
15. P. E. Stander, Cooperative hunting in lions: the role of the individual, *Behav. Ecol. Sociobiol.*, **29** (1992), 445–454. https://doi.org/10.1007/BF00170175
16. J. Duarte, C. Januário, N. Martins, J. Sardanyés, Chaos and crises in a model for cooperative hunting: a symbolic dynamics approach, *Chaos*, **19** (2009), 043102. https://doi.org/10.1063/1.3243924
17. L. Berec, Impacts of foraging facilitation among predators on predator-prey dynamics, *Bull. Math. Biol.*, **72** (2010), 94–121. https://doi.org/10.1007/s11538-009-9439-1

18. S. Saha, G. P. Samanta, Analysis of a tri-trophic food chain model with fear effect incorporating prey refuge, *Filomat*, **35** (2021), 4971–4999. https://doi.org/10.2298/FIL2115971S

19. S. Saha, G. P. Samanta, A prey-predator system with disease in prey and cooperative hunting strategy in predator, *J. Phys. A: Math. Theor.*, **53** (2020), 485601. https://doi.org/10.1088/1751-8121/abbc7b

20. M. T. Alves, F. M. Hilker, Hunting cooperation and Allee effects in predators, *J. Theor. Biol.*, **419** (2017), 13–22. https://doi.org/10.1016/j.jtbi.2017.02.002

21. A. J. Kashyap, Q. Zhu, H. K. Sarmah, D. Bhattacharjee, Dynamical study of a predator–prey system with Michaelis–Menten type predator-harvesting, *Int. J. Biomath.*, **16** (2023), 2250135. https://doi.org/10.1142/S1793524522501352

22. J. S. Tener, *Muskoxen in Canada: a biological and taxonomic review*, Ottawa: Queen's Printer, 1965.

23. W. Cresswell, J. Quinn, Faced with a choice, sparrowhawks more often attack the more vulnerable prey group, *Oikos*, **104** (2004), 71–76. https://doi.org/10.1111/j.0030-1299.2004.12814.x

24. J. Krause, J. G. J. Godin, Predator preferences for attacking particular prey group sizes: consequences for predator hunting success and prey predation risk, *Anim. Behav.*, **50** (1995), 465–473. https://doi.org/10.1006/anbe.1995.0260

25. D. Scheel, Profitability, encounter rates, and prey choice of African lions, *Behav. Ecol.*, **4** (1993), 90–97. https://doi.org/10.1093/beheco/4.1.90

26. M. Ono, T. Igarashi, E. Ohno, M. Sasaki, Unusual thermal defence by a honeybee against mass attack by hornets, *Nature*, **377** (1995), 334–336. https://doi.org/10.1038/377334a0

27. H. I. Freedman, G. S. K. Wolkowicz, Predator-prey systems with group defence: the paradox of enrichment revisited, *J. Math. Biol.*, **48** (1986), 493–508. https://doi.org/10.1007/BF02462320

28. J. F. Andrews, A mathematical model for the continuous culture of microorganisms utilizing inhibitory substrates, *Biotechnol. Bioeng.*, **10** (1968), 707–723. https://doi.org/10.1002/bit.260100602

29. V. Ajraldi, M. Pittavino, E. Venturino, Modeling herd behavior in population systems, *Nonlinear Anal.: Real World Appl.*, **12** (2011), 2319–2338. https://doi.org/10.1016/j.nonrwa.2011.02.002

30. E. Venturino, A minimal model for ecoepidemics with group defense, *J. Biol. Syst.*, **19** (2011), 763–785. https://doi.org/10.1142/S0218339011004184

31. M. Griesser, T. N. Suzuki, Naive juveniles are more likely to become breeders after witnessing predator mobbing, *Am. Nat.*, **189** (2017), 58–66. https://doi.org/10.1086/689477

32. P. Panday, N. Pal, S. Samanta, P. Tryjanowski, J. Chattopadhyay, Dynamics of a stage-structured predator-prey model: cost and benefit of fear-induced group defense, *J. Theor. Biol.*, **528** (2021), 110846. https://doi.org/10.1016/j.jtbi.2021.110846

33. P. Panja, S. Jana, S. K. Mondal, Dynamics of a stage structure prey-predator model with ratio-dependent functional response and anti-predator behavior of adult prey, *Numer. Algebra Control Optim.*, **11** (2021), 391–405. https://doi.org/10.3934/naco.2020033

34. Y. Du, B. Niu, J. Wei, A predator-prey model with cooperative hunting in the predator and group defense in the prey, *Discrete Contin. Dyn. Syst.-B*, **27** (2022), 5845–5881. https://doi.org/10.3934/dcdsb.2021298

35. S. Roy, P. K. Tiwari, H. Nayak, M. Martcheva, Effects of fear, refuge and hunting cooperation in a seasonally forced eco-epidemic model with selective predation, *Eur. Phys. J. Plus*, **137** (2022), 528. https://doi.org/10.1140/epjp/s13360-022-02751-2

36. S. Biswas, P. K. Tiwari, S. Pal, Delay-induced chaos and its possible control in a seasonally forced eco-epidemiological model with fear effect and predator switching, *Nonlinear Dyn.*, **104** (2021), 2901–2930. https://doi.org/10.1007/s11071-021-06396-1

37. S. S. Maity, P. K. Tiwari, S. Pal, An ecoepidemic seasonally forced model for the combined effects of fear, additional foods and selective predation, *J. Biol. Syst.*, **30** (2022), 285–321. https://doi.org/10.1142/S0218339022500103

38. P. Abrams, The hydra effect is no myth, *New Sci.*, **226** (2015), 28–29. https://doi.org/10.1016/S0262-4079(15)30463-2

39. P. A. Abrams, H. Matsuda, The effect of adaptive change in the prey on the dynamics of an exploited predator population, *Can. J. Fish. Aquat. Sci.*, **62** (2005), 758–766. https://doi.org/10.1139/f05-051

40. M. Sieber, F. M. Hilker, The hydra effect in predator-prey models, *J. Math. Biol.*, **64** (2012), 341–360. https://doi.org/10.1007/s00285-011-0416-6

41. H. Matsuda, P. A. Abrams, Effects of predator-prey interactions and adaptive change on sustainable yield, *Can. J. Fish. Aquat. Sci.*, **61** (2004), 175–184. https://doi.org/10.1139/f03-147

42. A. Schröder, A. van Leeuwen, T. C. Cameron, When less is more: positive population-level effects of mortality, *Trends Ecol. Evol.*, **29** (2014), 614–624. https://doi.org/10.1016/j.tree.2014.08.006

43. P. A. Abrams, C. Quince, The impact of mortality on predator population size and stability in systems with stage-structured prey, *Theor. Popul. Biol.*, **68** (2005), 253–266. https://doi.org/10.1016/j.tpb.2005.05.004

44. G. Birkhoff, G. C. Rota, *Ordinary differential equations*, 4 Eds., John Wiley & Sons, 1989.

45. L. Perko, *Differential equations and dynamical systems*, Springer, 2001. https://doi.org/10.1007/978-1-4613-0003-8

46. A. Dhooge, W. Govaerts, Y. A. Kuznetsov, H. G. E. Meijer, B. Sautois, New features of the software MatCont for bifurcation analysis of dynamical systems, *Math. Comput. Model. Dyn. Syst.*, **14** (2008), 147–175. https://doi.org/10.1080/13873950701742754

AIMS Press